Supplementary

Source apportionment of the submicron organic aerosols over the Atlantic Ocean from 53 °N to 53 °S using HR-ToF-AMS

Shan Huang[1,2,*,†], Zhijun Wu[3,†], Laurent Poulain[2,*], Manuela van Pinxteren[2], Maik Merkel[2], Denise Assmann[2], Hartmut Herrmann[2], Alfred Wiedensohler[2]

[1]Institute for Environmental and Climate Research, Jinan University, Guangzhou, 511443, China

[2]Leibniz Institute for Tropospheric Research, Leipzig, 04318, Germany

[3]College of Environmental Sciences and Engineering, Peking University, Beijing, 100871, China

Correspondence to: Laurent Poulain (poulain@tropos.de),

Shan Huang (shanhuang_eci@jnu.edu.cn)

Table S1 The boundary of latitude for each air mass group in the four cruises (unit: °).

Air mass group	**CR1**	**CR2**	**CR3**	**CR4**
Continent Europe **(Ec)**	25< Ec≤38.5	45.5< Ec≤51	45.5< Ec≤51	40 < Ec≤51
Marine Europe **(Em)**	38.5< Em≤48 15< Em≤25	30< Em≤45.5	20< Em≤45.5	31< Em≤40 19< Em≤ 25
Continent Africa **(Ac)**	6< Ac≤15	5< Ac≤30	3.5< Ac≤20	25< Ac≤31 10< Ac≤19
Marine Africa **(Am)**	-25< Am≤6	-32< Am≤5	-31< Am≤3.5	-33< Am≤10
Continent South Africa **(SAc)**	-	-	-55< Am≤ -31	-

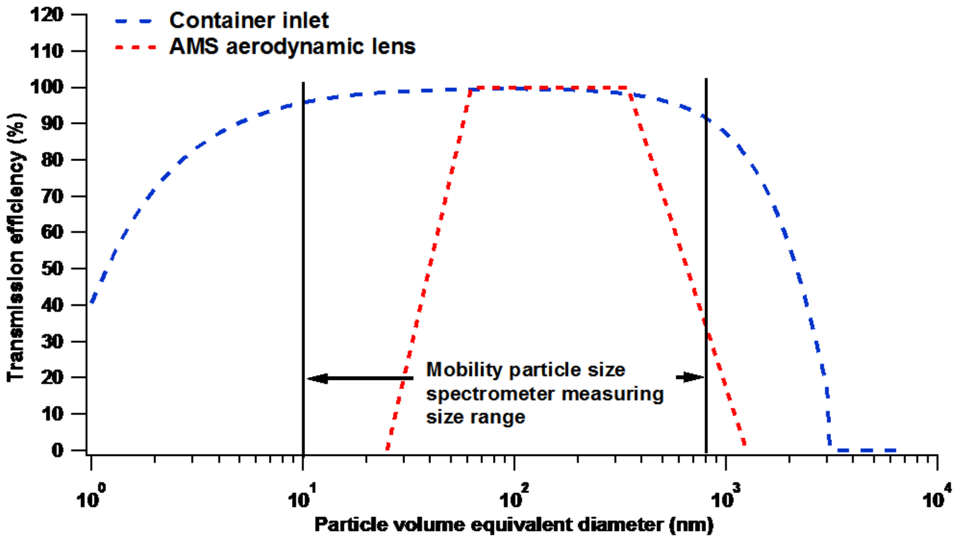

Figure S1 The transmission efficiency as a function of particle volume equivalent diameter for: the Aerosol container inlet (blue dashed line) derived by the Particle Loss Calculator (von der Weiden et al., 2009), and AMS aerodynamic lens (red dashed line) shown as an average of of transmission efficiency curves in several studies (Bahreini et al., 2008; Jayne, 2000; Takegawa et al., 2009; Zhang et al., 2004). The measuring size range of the mobility particle size spectrometer is depicted.

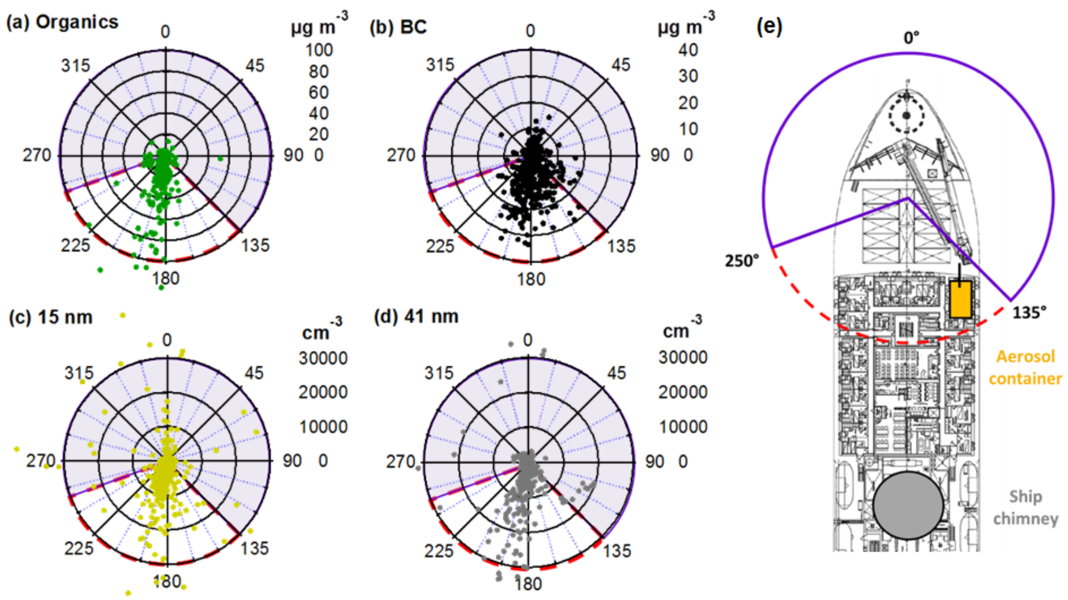

Figure S2 Wind rose (on relative wind direction, RWD) of mass concentration of (a) organics and (b) BC, as well as particle number concentration at size of (c) 15nm, and (d) 41nm. Data points are for CR4 at 20-min time resolution. (e) Location of Aerosol container and ship chimney, as well as the identified ship contamination range from 135 °to 250 °of RWD.

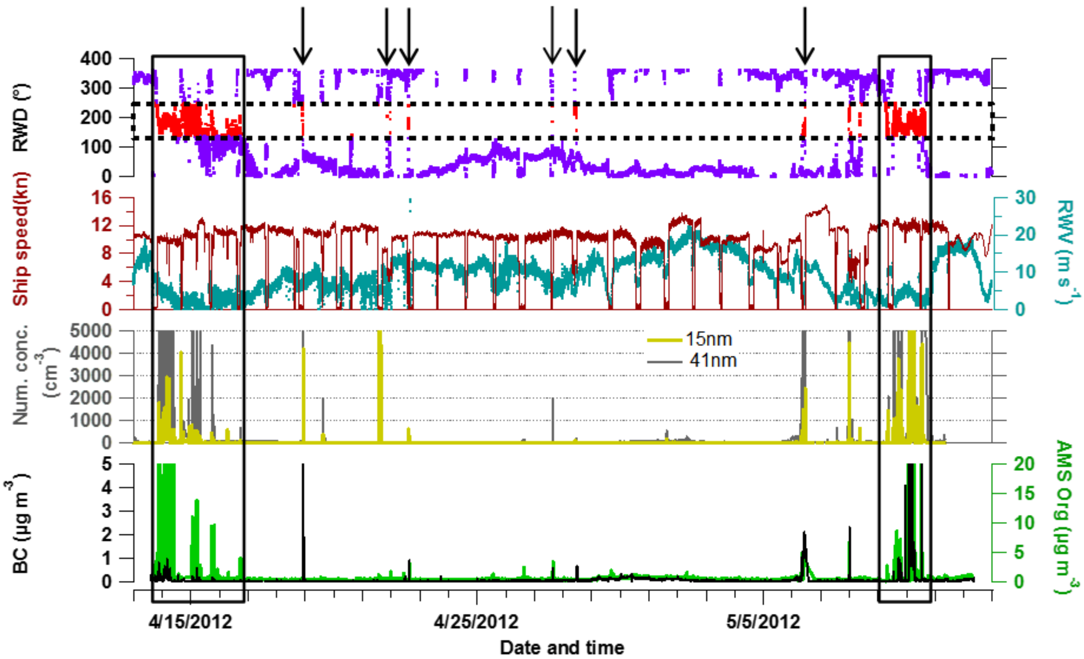

Figure S3 Example of CR3: unfiltered time series for mass concentration of organics (AMS) and BC (MAAP) and particle number concentration (Num. conc.) of 15 nm and 41 nm particles, together with relative wind direction (RWD), relative wind velocity (RWV) and ship speed.

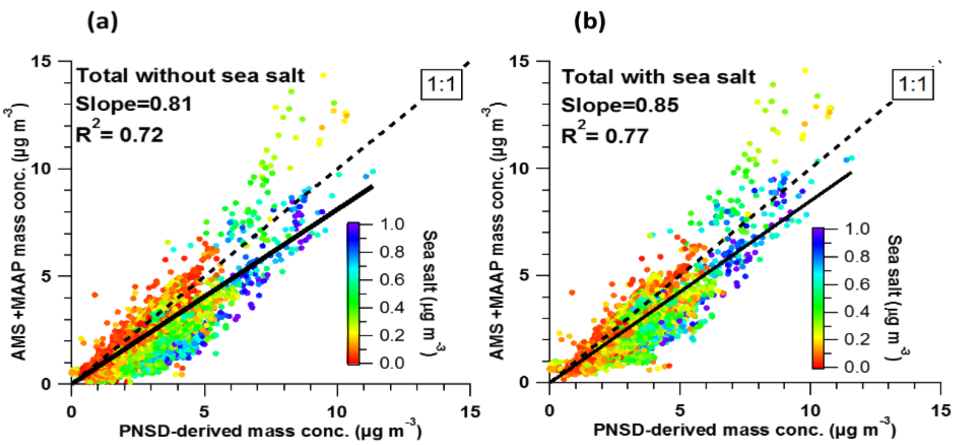

Figure S4 Correlation between total particle mass concentration from AMS + MAAP (a) without sea salt and (b) with sea salt to that derived from particle number size distribution (PNSD), coloured by mass concentration of sea salt. Note that to derive the density of the particles the following densities have been used for individual species: 1.75 g cm^{-3} for sulfate, nitrate and ammonium, 1.4 g cm^{-3} for organics, 1.52 g cm^{-3} for chloride, 1.77 g cm^{-3} for BC and 2.17 g cm^{-3} for the sea salt. CE = 0.7 is chosen and applied.

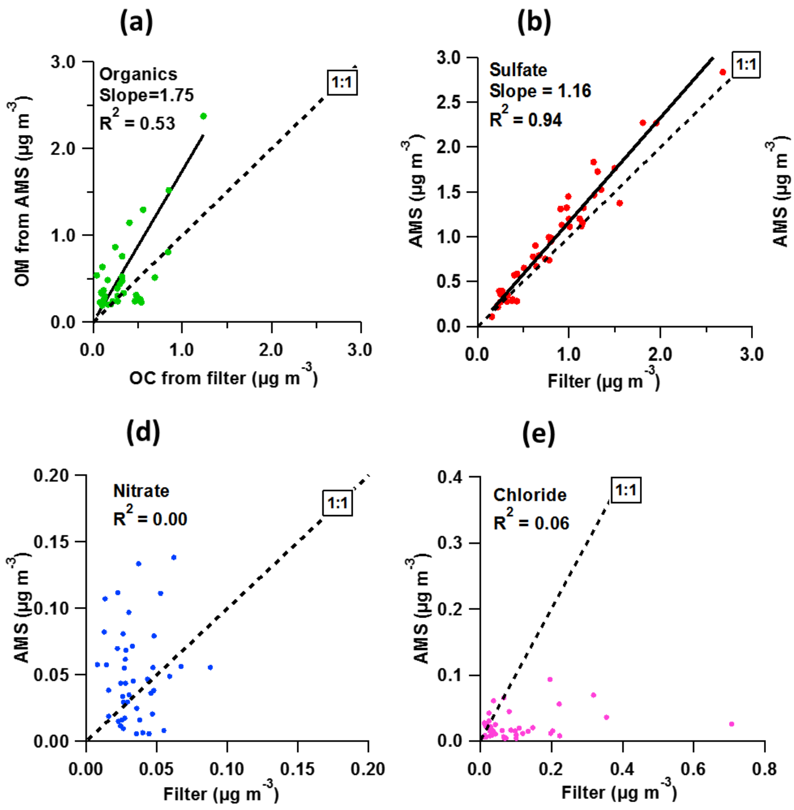

Figure S5 Comparison between AMS measurements and filter measurements for (a) organics (organic matters, OM, vs organic carbon, OC), (b) sulfate (c) ammonium (d) nitrate and (e) chloride during Polarstern cruises.

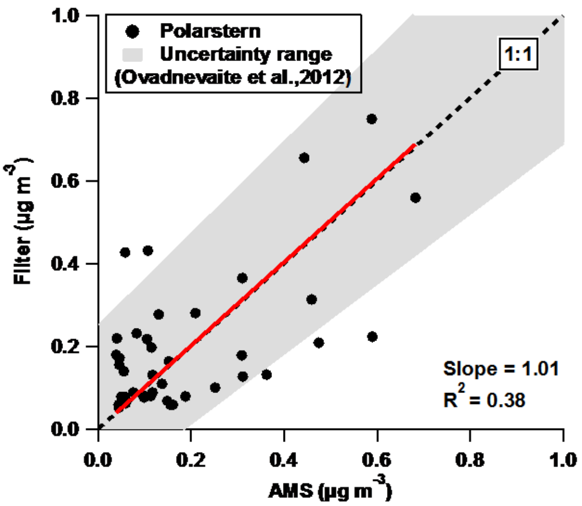

Figure S6 Comparison between sea salt mass concentrations from filter measurements and AMS measurements during Polarstern cruises. The grey shadow presents the uncertainty range of the similar comparison at Mace Head, adapted from Ovadnevaite et al. (2012).

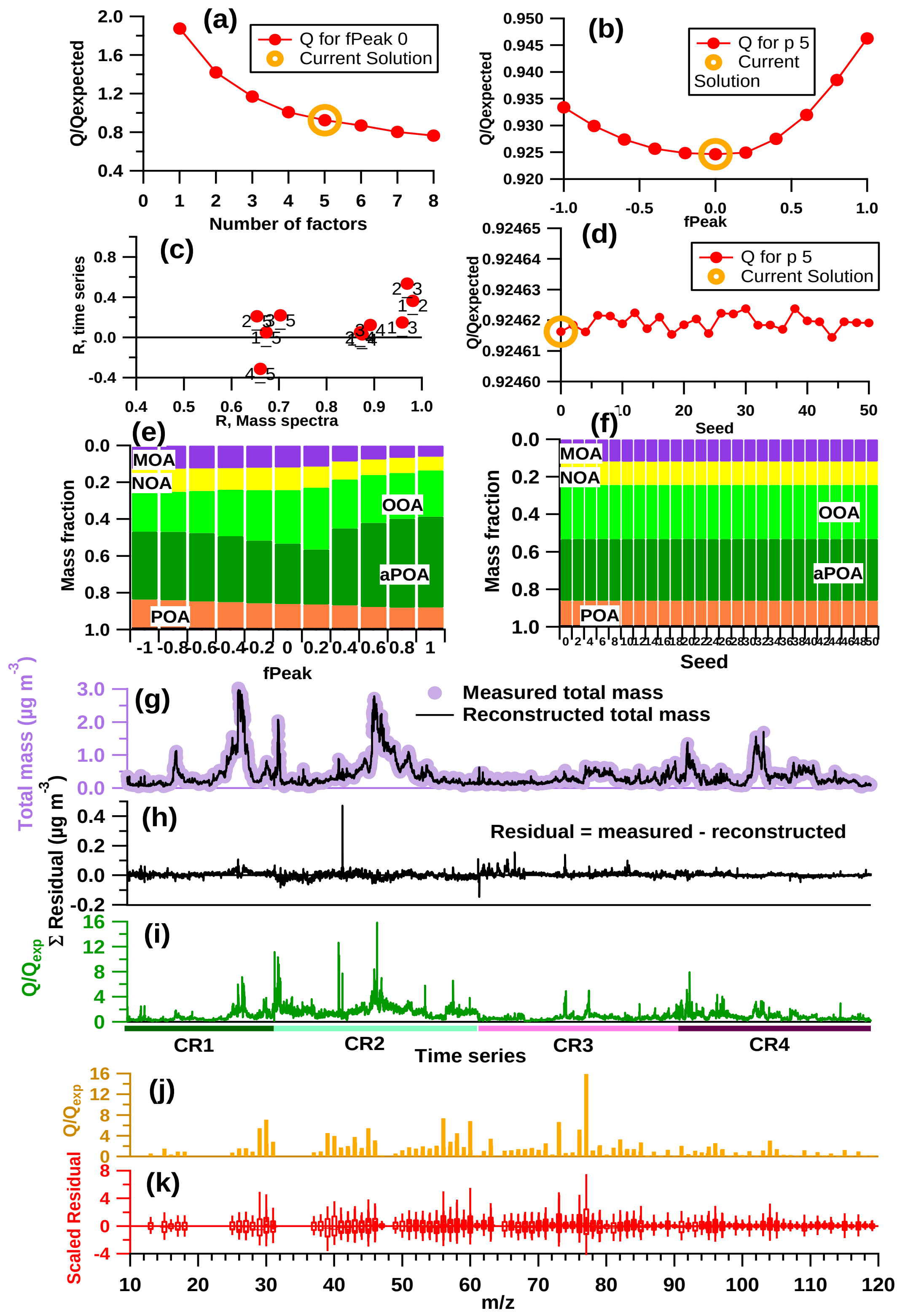

Figure S7 Diagnostic plots: (a) Q/Q_{exp} ratio vs. number of factors, (b) Q/Q_{exp} vs. fPeak between -1 and 1 in step of 0.2 for 5-factor solution, (c) Pearson's correlation coefficient R for time series and mass spectra among 5 factors, (d) Q/Q_{exp} vs. seeds between 0 to 50 in step of 2, (e) variation of mass fraction of each factor as a function of fPeak, (f) variation of mass fraction of each factor as a function of seeds, (g) comparison of total measured mass and reconstructed mass, (h) sum of the residuals of the fit, (i) Q/Q_{exp} in time series, (j) Q/Q_{exp} for each m/z, and (k) scaled residuals for each m/z, with horizontal bars for median, boxes for interquartile and sticks for 95% and 5% of points.

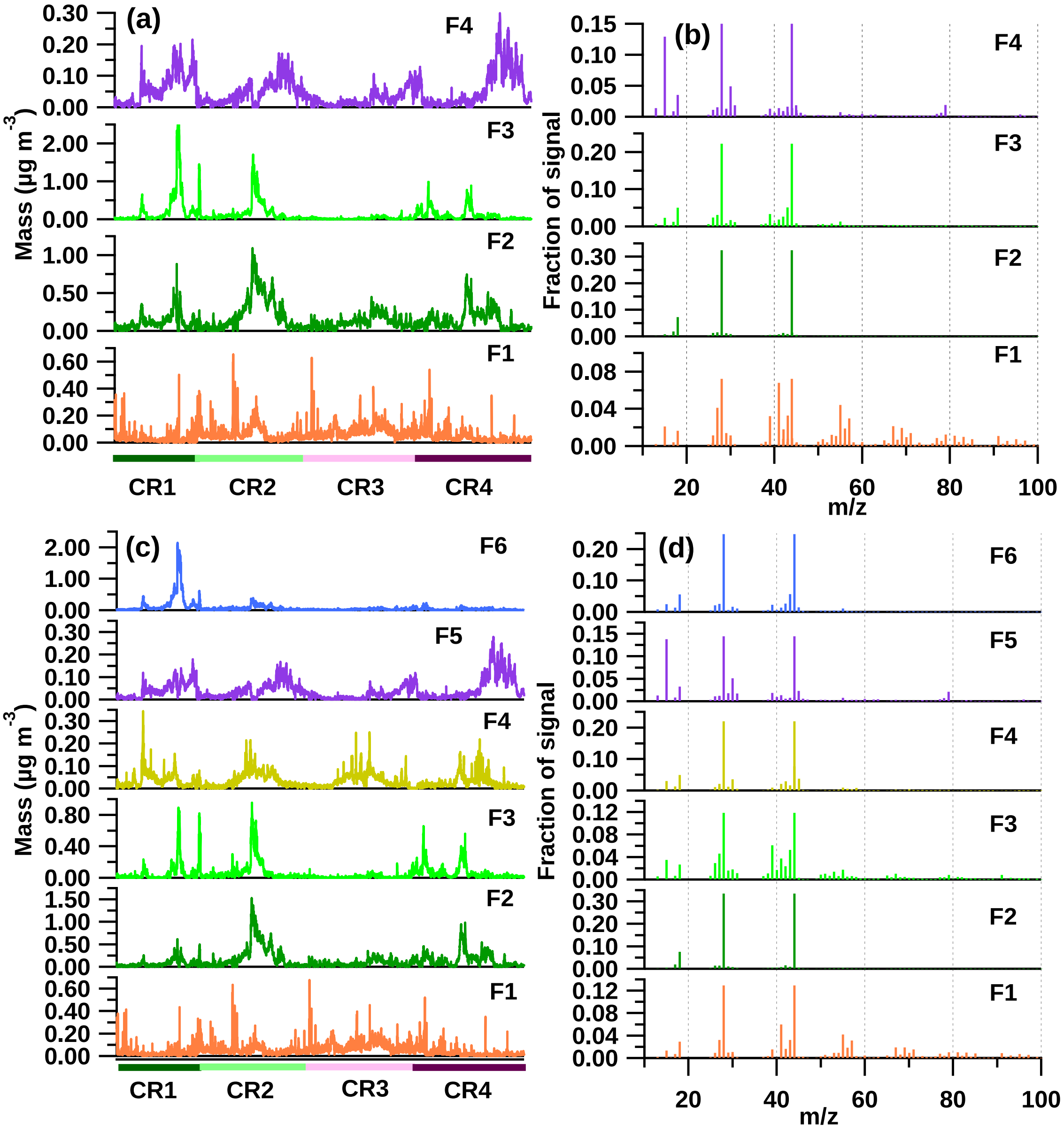

Figure S8 Time series and mass spectra for OA components of (a, b) 4-factor solution, (c, d) 6-factor solution.

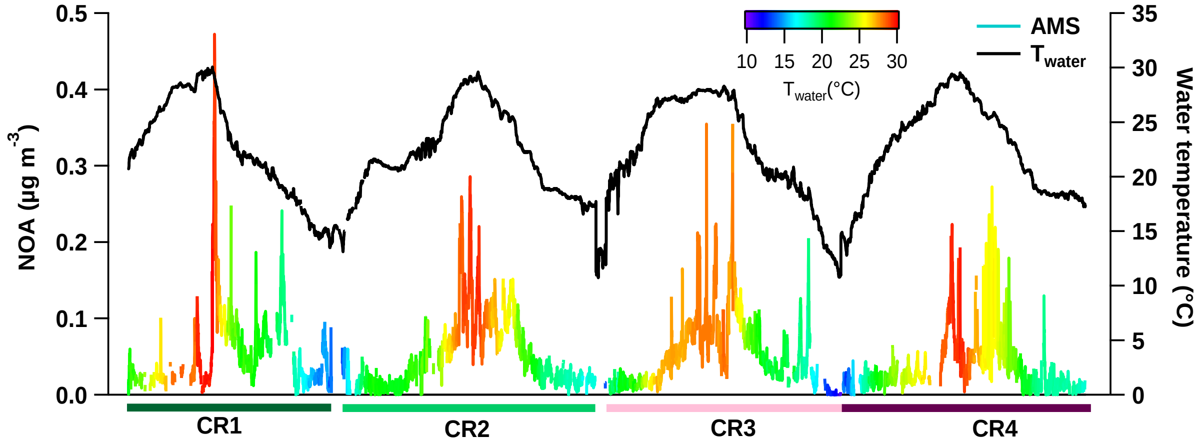

Figure S9 Similar variation between water temperature and NOA (also colored in water temperature) during 4 cruises.

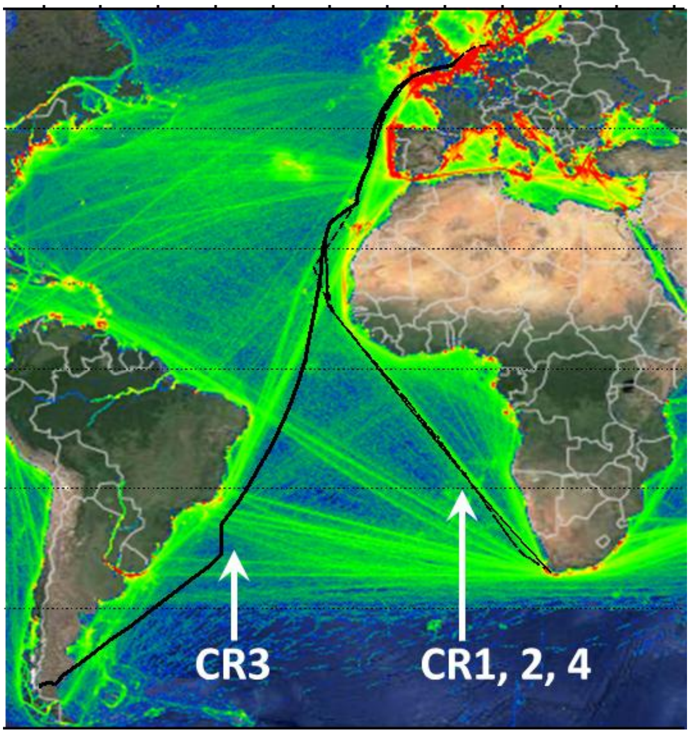

Figure S10 Density map of the maritime traffic with Polarstern cruise tracks (black lines). The background snapshot was taken from https://www.marinetraffic.com/en/ on May 2014 and assumed to be similar to the situation in 2011 and 2012.

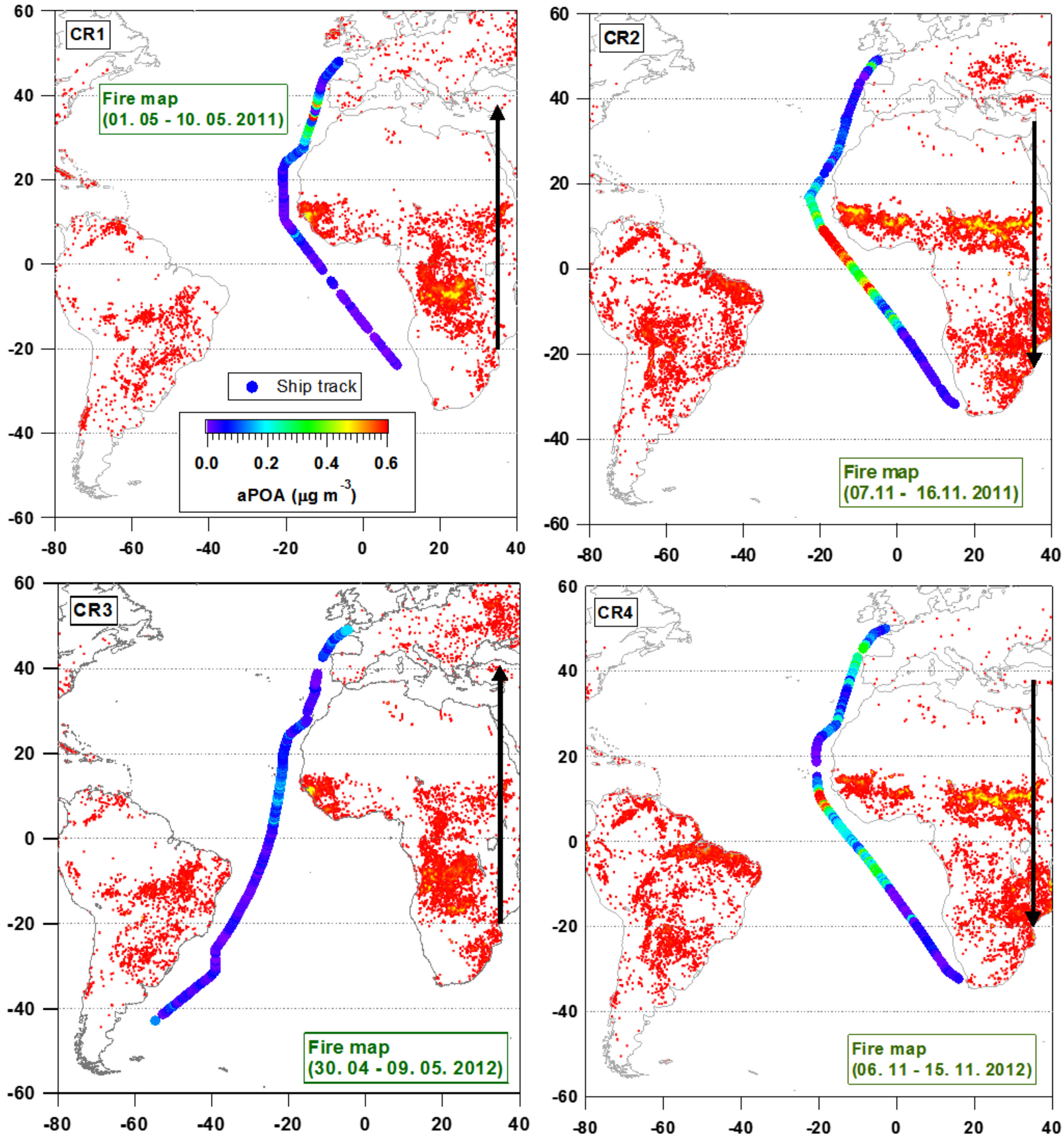

Figure S11 Fire maps obtained from an online database of MODIS satellite (http://rapidfire.sci.gsfc.nasa.gov/firemaps/) , colored by aPOA mass concentration during Polarstern cruises. The black arrows show the ship direction.

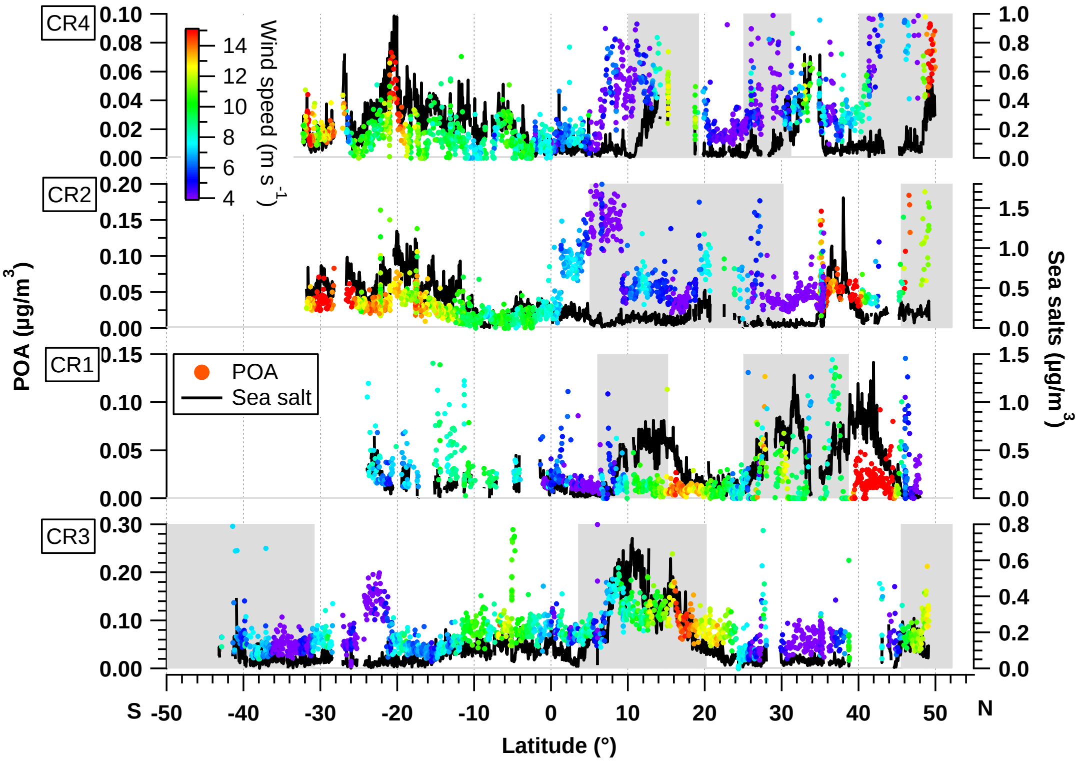

Figure S12 Latitude distribution of POA mass concentration (left axis), comparing to the sea salt particle mass concentration (right axis). The POA is colored by wind speed (true wind speed). Red boxes mark the cases in which the POA and estimated sea salt show similar variation. Grey background indicates continental air masses, white one for marine air masses

References

von der Weiden, S. L., Drewnick, F., & Borrmann, S. (2009). Particle Loss Calculator – a new software tool for the assessment of the performance of aerosol inlet systems. *Atmos. Meas. Tech.*, *2*(2), 479-494.